TECHNICAL UNIVERSITY OF CLUJ-NAPOCA

ACTA TECHNICA NAPOCENSIS

Series: Applied Mathematics, Mechanics, and Engineering
Vol. 68, Issue III, September, 2025

BIOMECHANICAL RESPONSE OF A LEFT DELTOID MODEL TO BOWEN TECHNIQUE STIMULI

Adrian - Ioan BOTEAN, Dan Marius GHERASIM, Mariana ARGHIR

Abstract: *This study analyzes the distribution of mechanical stresses in the left deltoid muscle using photoelasticimetry, an advanced experimental method based on the accidental birefringence property of optically active materials. Anatomical models made of epoxy resin (EP14NV) were fabricated to replicate healthy human geometry, simulating manual stimuli from Bowen therapy. Three rigid models (M1–M3) were statically loaded (13.42–28.12 N), and stress fields were analyzed using a circular polarization polariscope. The results revealed distinct isochromatic fringe patterns, quantitatively correlating load magnitude with stress propagation in the anterior/posterior fascicles. While the study confirms the utility of photoelasticity in biomechanical modeling, limitations such as the absence of real viscoelasticity highlight the need for model refinement. The results demonstrate a direct correlation between load magnitude and stress propagation in the anterior/posterior fascicles, suggesting optimal force ranges for Bowen Therapy applications. This validates photoelasticimetry as a tool for non-invasive therapy assessment. This research opens new perspectives in the assessment of non-invasive muscle therapies.*

1. INTRODUCTION

This study employs photoelasticimetry [1-3] to investigate stress [4-6] propagation patterns within the left deltoid muscle under simulated Bowen Therapy loading conditions. The experimental approach utilizes epoxy resin anatomical models [7] that accurately replicate human muscular geometry, enabling quantitative analysis of principal stress (σ_1) distribution.

The study focuses on the preliminary phase of creating physical models from epoxy resin [7], manufactured to accurately replicate the anatomy of a healthy human subject's deltoid muscle. The modeling process involves careful material selection, such as EP 14NV epoxy, and the production of anatomical models through silicone mold casting, ensuring precise representation of muscular geometry. These models are then prepared for photoelasticimetric analysis, which will highlight stress distribution under simulated loading conditions inspired by Bowen technique manual interventions.

The study employs three identical rigid physical models (M1, M2, M3) [7] of the left deltoid muscle, designed to accurately replicate human geometric anatomy.

These models enable both qualitative and quantitative analysis of principal stress (σ_1) distribution under static loading conditions induced by Bowen Therapy - specific manipulations, using photoelasticimetry. Through this experimental approach, the research aims to provide mechanistic insights into the interactions between applied forces and the musculo-fascial structure.

Bowen Therapy (Bowtech/Bowenwork [8]), originated by Australian practitioner Tom Bowen in the ‘50s, employs specialized manual techniques addressing the fascial system through precisely controlled pressures interspersed with therapeutic intervals. Its hallmark is the delivery of targeted mechanical stimuli at defined anatomical locations, followed by mandatory recovery periods facilitating physiological integration.

Bowen Therapy is a non-invasive manual approach, wich can be considered a form of mechanotherapy [9-11], characterized by the controlled application of mechanical stimuli to soft tissues. This therapeutic technique is distinguished by its strategic use of tensile,

Received: 20.07.25; **Similarities**: 01.09.25: **Reviewed**: 02.09./05.09.25: **ccepted**:11.09.25.

compressive, and torsional forces, systematically alternated with therapeutic pauses of at least two minutes - a critical duration for the body's processing of mechanical signals.

Mechanical loading in Bowen Therapy spans a continuum from low-intensity, slow-oscillation stimuli to high-velocity manipulations, strategically modulated per therapeutic objectives. Application follows topographical anatomical mapping, with force vectors and kinetics optimized for tissue-specific viscoelastic properties [12].

The mechanical interventions of Bowen Therapy act upon a broad spectrum of anatomical structures, including the tegumentary layer, musculo-tendinous system, ligamentous apparatus, articular elements, and neural components, eliciting a complex therapeutic response [12-15]. Within the context of mechanotherapies, these mechanical stimuli trigger two complementary physiological regulatory mechanisms. The homeostatic response occurs at all levels of the human system/organism.

The first mechanism, known as mechanotransduction, involves biophysical and biochemical processes at tissue, cellular, and molecular levels [16], while the second mechanism entails signal transmission through the central and autonomic nervous systems, ensuring an integrated whole-body response. In both regulatory processes, fascia plays an essential functional role [17], serving as both a structural and informational mediator between various components of the myofascial system.

The sensory activation phase involves applying extremely light pressure (<0.5 N) to the tegumentary layer, with precise skin displacement without sliding. This initial maneuver typically focuses on the ventral region of the target muscle, selectively engaging the superficial fascia. The movement is performed in a transverse plane relative to the muscle fiber orientation.

The fascial challenge phase constitutes the core therapeutic intervention, involving firm transverse pressure application (3-5 N) directed opposite to the initial tissue displacement. Maintained for 3-10 seconds according to specific protocol requirements [13], this maneuver induces controlled deformation of the deep fascia, creating precisely localized static mechanical stresses.

Performed in immediate succession to fascial challenge, the transverse rolling technique applies similar directional loading with modified velocity profiles before abrupt tissue release, producing precisely tuned mechanical waves (0.5-2 Hz) that transmit therapeutic stimuli to periarticular structures through viscoelastic coupling.

The therapeutic pause, lasting a minimum of 2 minutes, represents the essential component for procedural integration. This interval facilitates both local signal processing through mechanotransduction and the coordinated response of the central and autonomic nervous systems at the organism level.

In its specific application to the left deltoid muscle, the Bowen Technique induces structural modifications through the combined action of tensile, compressive, and torsional forces. These mechanical stimuli cause a redistribution of the center of mass within the anterior and posterior muscle fascicles, with direct implications for regional biomechanics.

We hypothesize that: stress patterns in the deltoid are asymmetric under Bowen-type loads, with higher concentrations in the posterior fascicles; the epoxy resin model can replicate key mechanical interactions despite lacking viscoelasticity.

Figure 1 documents the deltoid-specific therapeutic sequence, illustrating both the posterior deltoid fascial challenge maneuver (Fig. 1a) and the anterior deltoid challenge fase technique (Fig. 1b).

2. MATERIAL AND METHODS

For this study, the proposed objective necessitated the implementation of a complex methodological process focused on structural analysis of the left deltoid muscle under Bowen Therapy conditions. The procedure involved: (1) acquisition of a standard anatomical model of the left arm region, followed by (2) development of customized epoxy resin replicas designed to accurately reproduce muscular anatomy.

Subsequently, we performed experimental simulation of the mechanical loads induced by the therapeutic intervention, with precise mapping of their distribution within the discrete muscular structure. For experimental validation, the models were transversely sectioned, and the resulting surfaces underwent meticulous preparation for analysis using transmission polariscopy. This approach enabled precise mapping of stress fields, visualized through isochromatic fringe patterns, thereby providing microscopic-scale insight into the therapy's effects on muscular behavior.

a)

b)

Fig.1. Bowen therapy shoulder protocol: a) Posterior deltoid challenge technique; b) Anterior deltoid challenge maneuver.

To thoroughly investigate the effects of static loading on the muscle model's structure, we developed anatomical models from transparent epoxy resin. This material was selected due to its exceptional optical properties, which make it ideally suited for studying stress distribution mechanisms.

The transparent epoxy resin exhibits the ability to record and retain mechanical stresses within its structure following external loading—a phenomenon known as residual stresses. Consequently, this material enables both real-time visualization of stress fields and their preservation for subsequent analysis.

This optical technique enables the quantification and interpretation of internal stress distributions through analysis of polarized light interference patterns, thereby providing critical insights into the material's structural behavior under static loading conditions [7, 18].

Thus, the use of transparent epoxy resin as a muscle modeling medium provides an innovative approach to photoelastic analysis, enabling deeper understanding of stress transmission mechanisms in simulated biological structures.

The initial stages of left deltoid muscle modeling—including reconstruction of its anatomical geometry and insertion points—were detailed in our previous work [7], as illustrated in Figures 2 and 3. What follows is a description of subsequent muscle model replication stages, with particular focus on:

Fig.2. Reference model.

Fig.3. Anatomical models fabricated in epoxy resin.

To accurately replicate the muscular structure, epoxy resin was selected as the photoelastic (optically active) material due to its key properties: in an unstressed state, the material is isotropic and fully transparent, enabling clear observation of internal structures; under external mechanical loading, the epoxy resin exhibits birefringence, becoming optically anisotropic. This behavior allows for the visualization and quantitative assessment of stress fields using photoelastic techniques.

The two-component epoxy resin EP14 NV was chosen based on the following characteristics: polymerization time: 48 hours, ensuring gradual and uniform curing without inducing residual stresses prior to testing; high mechanical and optical stability, which is critical for generating accurate and reproducible models.

This material selection enables not only the anatomical replication of the deltoid muscle but also qualitative analysis of stress distribution via advanced optical techniques, such as photoelasticity. Subsequent phases of the study will address the casting process, specimen conditioning, and the mechanical loading methodology for structural behavior assessment.

The structural modeling of the left deltoid muscle and its insertions involved a complex approach, beginning with the fabrication of two 18-mm-thick MDF boxes, specifically sized for each insertion area: 100×100×90 mm for the humerus and 150×175×90 mm for the anterior clavicular margin, acromion, and scapular spine. The casting process was performed in successive stages, starting with a 10-mm-thick base layer of epoxy resin that served as a support for fixing the muscle models, as shown in Figure 4.

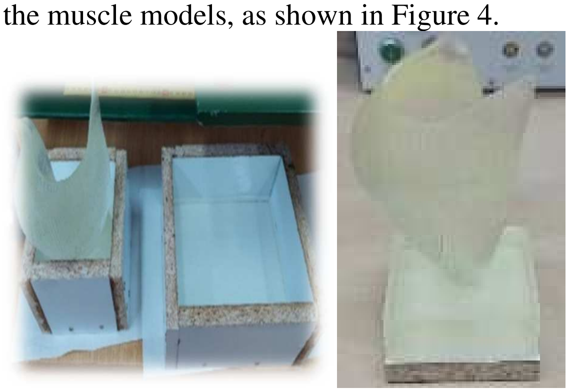

Fig.4. Modeling the insertions through casting in MDF molds.

Through controlled, iterative casting techniques, three unitary bodies (M1, M2, and M3) of the left deltoid were fabricated, each seamlessly integrating the corresponding anatomical insertions (Figure 5). This methodology ensured not only anatomical precision and structural consistency but also optimal compatibility with photoelasticity techniques, enabling visualization and analysis of stress fields under mechanical loading.

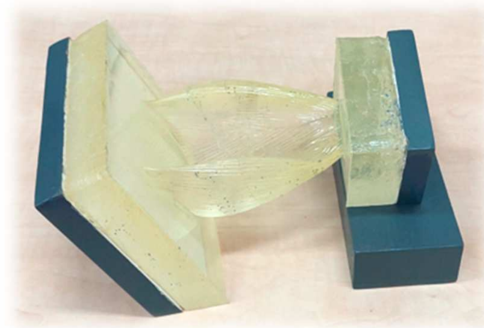

Fig.5. Final prototype.

The modeling process for the unitary bodies of the left deltoid employed an artisanal approach, with each model individually fabricated through manual casting techniques. While this methodology resulted in geometric variations among the three resulting specimens (M1, M2, and M3), it effectively replicates the inherent anatomical complexity of muscular structures. Each model exhibits unique characteristics regarding insertion configuration on the acromion, clavicle, and scapular spine, thereby reproducing the natural variability between different anatomical subjects.

The geometric variations between models do not compromise the study's validity, but rather provide a more comprehensive perspective on muscular behavior. Each unitary body functions as an independent system, maintaining internal consistency in both stress distribution and mechanical response to loading. This approach enables comparative analysis of how anatomical variations influence force transmission within the deltoid complex.

Moreover, each model's individual characteristics align with fundamental biomechanical principles, where no anatomical structure is perfectly identical. Thus, the study benefits from structural diversity that enhances the photoelastic analysis, enabling observation of a broader spectrum of potential mechanical behaviors in the deltoid muscle under loading conditions.

To replicate the biomechanical loading conditions of the left deltoid, a modular experimental system was developed (Figs. 6-8). Constructed from beech wood and based on an optimized lever mechanism, the system incorporated three distinct configurations for models M1-M3 (Figs. 9-11).

The loading system employs a platform with a base mass of 370 g, subjected to incremental weight progression. For model M1 (designed for posterior deltoid analysis), the total applied load was 1,370 g (1,000 g additional), generating a force G_1 = 13.42 N (Fig.12). Models M2 (posterior deltoid) and M3 (anterior deltoid) were identically calibrated to 2,870 g loads, corresponding to forces $G_2 = G_3 = 28.12$ N (Figs. 13-14).

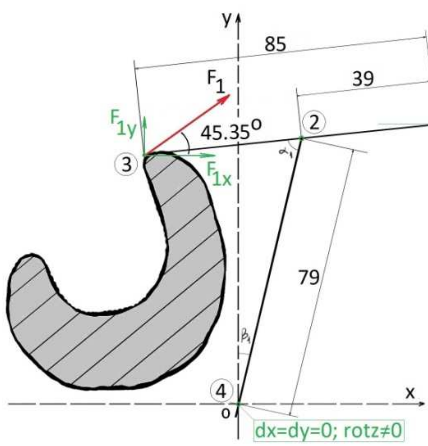

Fig.6. Loading configuration for posterior deltoid specimen M1 (cross-section) and test stand schematic.

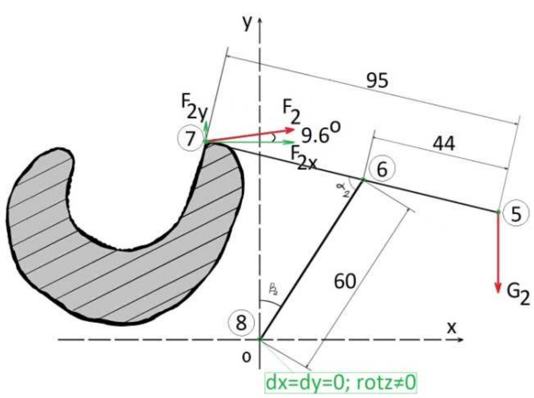

Fig.7. Loading configuration for posterior deltoid specimen M2 (cross-section) and test stand schematic.

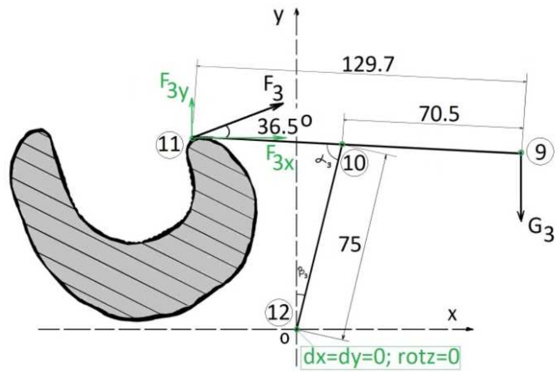

Fig.8. Loading configuration for posterior deltoid specimen M3 (cross-section) and test stand schematic.

To determine the stress distribution within the modeled structure, an advanced computational approach based on the finite element method was implemented. The mechanical system, characterized by its geometric configuration (Figs. 6–8), was analyzed under static conditions, assuming linear-elastic material properties and isotropic structural behavior.

Fig.9. Mechanical loading setup (M1) simulating posterior deltoid forces.

Fig.10. Posterior deltoid loading setup M2.

Fig.11. Loading rig M3 for the anterior deltoid.

The boundary conditions were defined according to a mixed support model, where nodes 3, 4, 7, 8, 11, and 12 had translation constraints along both Cartesian axes ($d_x = d_y = 0$) while permitting rotational freedom about the normal axis (rotz ≠ 0). These kinematic constraints provide a partially fixed condition, essential for proper modeling of stress transfer within the system.

Fig.12. M1 test setup in thermal conditioning chamber.

Fig.13. M2 test configuration in thermal conditioning chamber.

Fig.14. M3 test configuration in thermal conditioning chamber.

External forces G_1, G_2, and G_3 were applied at nodes 1, 5, and 9 respectively, with distinct magnitudes according to the specified loading scenarios. Following the fundamental principle of statics, these external actions induce reactions at nodes 3, 7, and 11 (denoted F_1, F_2, F_3), whose exact determination requires solving a statically indeterminate system.

The computational analysis was performed using the RDM 7.04 platform (Ossatures module), which implements advanced numerical solving algorithms for complex mechanical systems. Domain discretization employed beam finite elements characterized by constant stiffness and capable of transferring axial, shear, bending, and torsional loads. This modeling approach was justified by the problem's specific geometry and loading conditions.

The input geometric data (Table 1) provides a complete description of the nodal configuration required for mathematical model construction. The numerical solution obtained through this methodology enables both determination of reaction forces F_1, F_2, and F_3.

Table 1

Cartesian coordinates of the nodes used in the finite element analysis.

Nodes	x[mm]	y[mm]
1	127.49	101.49
2	88.43	97.6
3	42.83	92.57
4	70.09	20.6
5	159.55	65.46
6	116.67	75.73
7	67.15	87.81
8	84.06	25.24
9	217.7	106.4
10	146.89	109.42
11	88.14	111.68
12	129	36.72

In this numerical modeling study, the order of magnitude of reaction forces at nodes 3, 7, and 11 is of particular interest. Table 2 summarizes the obtained numerical results (consistent with Figures 6-8).

Table 2

Numerical results obtained for the loading forces acting on models M1, M2, and M3.

Nodes	F_x[N]	F_y[N]	F[N]
3	7.7	8.0	11.245
7	32.5	5.2	31.18
11	23.5	18	30.261

The thermo-stabilization process of the models involved a heat treatment at 80°C for 60 minutes, with maintained mechanical loading, followed by controlled cooling in the oven environment (Figs. 12-14). This protocol induced a structural reorganization through: the plasticization of residual stresses, with redistribution of internal loads; the stabilization of the deformed configuration, imprinting a mechanical "memory"; and the optimization of the elastic properties of the anatomical structure.

The post-thermal sample preparation process involved a precise methodology for marking and sectioning. After the heat treatment and removal from the experimental setup, the analysis sections were marked using a scribing caliper. These sectioning planes, oriented parallel to the direction of the applied force (as shown in Figure 15), allowed for the preservation of the deformed geometry acquired during thermo-mechanical loading, the identification of critical stress concentration zones, and the accuracy required for subsequent investigations of the internal structure.

Fig.15. The marking of parallel transverse sections.

The marking operation was carried out with special care to preserve the model's integrity and ensure the correlation between the stressed state and the final configuration. Orienting the sections along the direction of the applied force optimized the visualization of loading effects on the anatomical structure.

The mechanical processing of the samples was performed using high-precision manual techniques. The manual sectioning was followed by a sequence of finishing operations, including progressive grinding with increasing grit size (40-5,000) as shown in Figure 16, surface preparation to obtain optical analysis planes, and optimization of surface quality required for microstructural investigations.

Fig.16. The prepared cross-sections after cutting and grinding.

Each processing step was tailored to the material's specific characteristics while preserving the structural configuration acquired during thermo-mechanical treatment. The progressive grinding ensured the gradual removal of surface defects, achieving a finish suitable for subsequent analyses.

The analysis of transverse sections corresponding to the three models (M1, M2, and M3) is performed by positioning them in a circular polarization polariscope (light field configuration) using either a monochromatic light source (sodium lamp) or a white light source. The polariscope, manufactured by Tiedemann Instruments [19], is shown in Figure 17.

3. RESULTS

The analysis performed using the polariscope, in both white and monochromatic light, revealed the distribution of static stress states generated in the model sections as a result of stimuli induced by Bowen Therapy. The study detected these stress states in the sampled sections, along with their configuration in the loaded area and their propagation mechanism toward muscle insertions and adjacent anatomical structures. These stress states are identified in the sections through the shape of isochromatics and their fringe order [18].

Fig.17. The cross-sections were analyzed in the polariscope under white light illumination.

In white light, isochromatics manifest as colored fringes covering the entire chromatic spectrum resulting from white light decomposition. Under monochromatic illumination, they appear as dark fringes [1-3, 18, 20].

A comparison between models M1 and M2 reveals that isochromatic distribution is influenced by the intensity of external loading (G1 and G2, respectively). An increase in applied load leads to higher fringe orders, demonstrating a directly proportional relationship between the magnitude of mechanical stress and the model's optical characteristics.

The data regarding the number of recorded isochromatics for the posterior deltoid (models M1 and M2) and anterior deltoid (model M3) under static stress conditions are summarized in tabular form. These results highlight the variation in fringe order relative to the magnitude of applied loading.

The distribution of static stress states can be visualized through polarized light optical images, which reveal the isochromatic fringe patterns in the analyzed cross-sections. These images demonstrate both stress concentration in loaded areas and stress propagation toward muscle insertions and adjacent anatomical structures.

Furthermore, graphical representations of the stress distribution across sections enable quantitative analysis of isochromatic fringe order variation. The plots show a direct correlation between increasing external load and higher fringe orders, confirming the dependence between mechanical stress intensity and the material's optical response.

Table 3 presents a sequence of images showing the isochromatic fringe distribution across all 14 transverse sections (S) of model M1, under both monochromatic and white light illumination. These images clearly reveal the static stress state configurations, providing comprehensive visualization of stress propagation throughout the entire model volume.

Table 3

The distribution of isochromatics across the transverse sections comprising model M1.

S	Monochromatic light	White light
S1		
S2	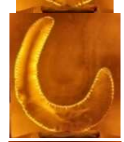	
S3	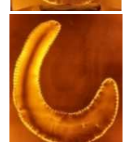	
S4		
S5	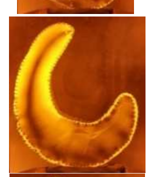	
S6	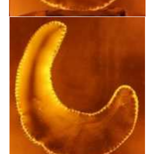	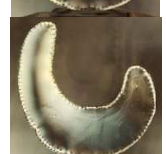
S7		

S8		
S9		
S10	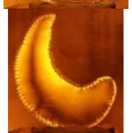	
S11	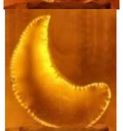	
S12		
S13		
S14		

For model M1 loaded according to the posterior deltoid stress pattern, the images primarily reveal only the isoclinic (showing the principal stress directions σ_1 and σ_2), while in section S4, an isochromatic fringe of order k=1 is recorded.

Table 4 presents a sequence of images illustrating the distribution of isochromatic fringes across the 11 transverse sections (S) of model M2, under both monochromatic and white light illumination.

Table 4

The distribution of isochromatics across the transverse sections comprising model M2.

S	Monochromatic light	White light
S1		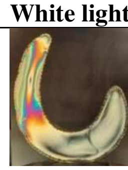
S2		
S3		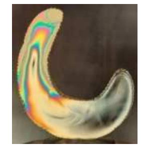
S4		
S5	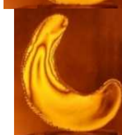	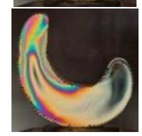
S6		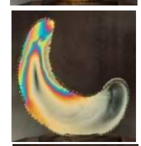
S7		
S8		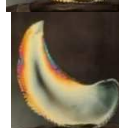
S9		
S10		
S11		

Table 5 shows a sequence of images depicting the isochromatic fringe distribution across all 11 transverse sections (S) of model M3, captured under both monochromatic and white light illumination.

Table 5

The distribution of isochromatics across the transverse sections comprising model M3.

S	White light	Monochromatic light
S1		
S2		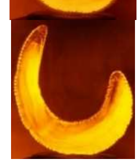

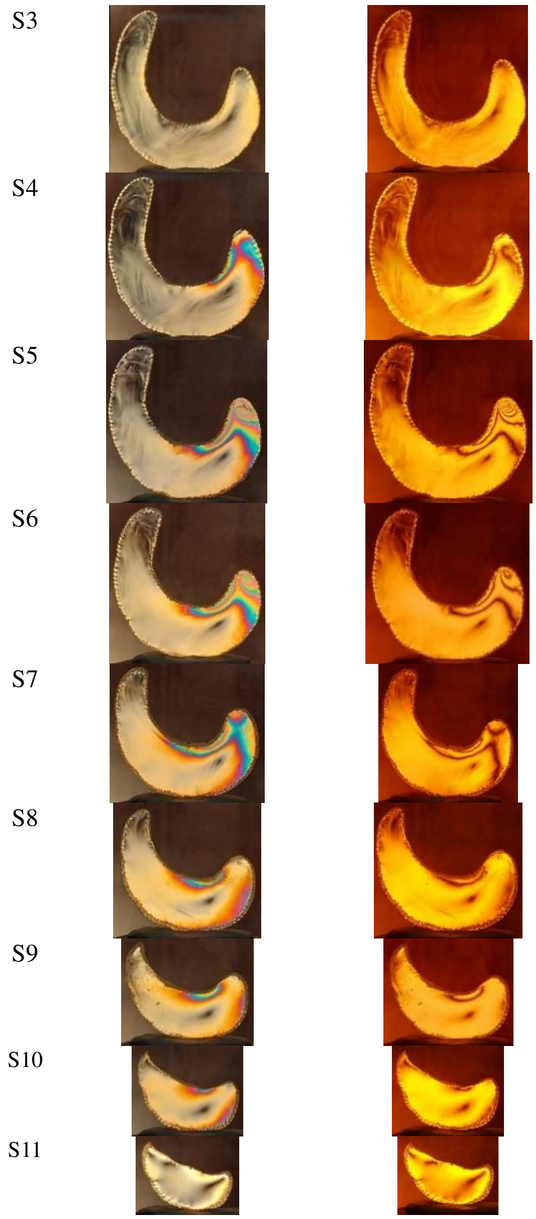

In accordance with Tables 4 and 5, the following graphs present the variation of isochromatic fringe order 4 in the transverse sections of models M2 and M3, as shown in Figures 18 and 19.

The marking operation was carried out with special care to preserve the model's integrity and ensure the correlation between the stressed state and the final configuration. Orienting the sections along the direction of the applied force optimized the visualization of loading effects on the anatomical structure.

This isolation of a biological component from its system fails to capture the complexity of its context—the surrounding structures and the whole to which it connects via continuous connective tissue receptors [21-23]—and represents a limitation of the present study.

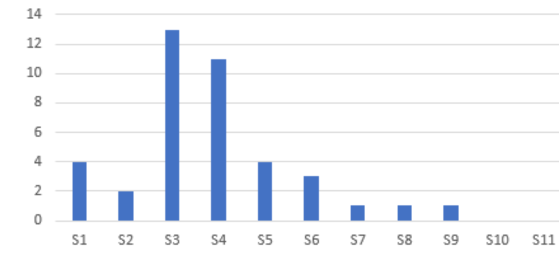

Fig.18. Graphical representation of isochromatic distribution in model M2.

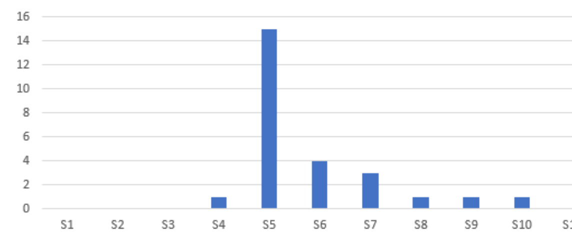

Fig.19. Graphical representation of isochromatic distribution in model M3.

However, reproducing all influences within an integrated systemic process, particularly in vivo, is currently impossible to fully model from a mechanical engineering standpoint. Thus, we focus here on investigating the behavior of an anatomical model of the left deltoid muscle during simulated mechanical stimuli induced by Bowen Therapy, while acknowledging its inherent limitations: arm displacement, post-loading muscle deformation, and the non-homogeneous nature of real muscle tissue where myofascial tensions vary with muscle ischemia or fascial adaptations [23].

Nevertheless, the stress states induced in the model are detected by mechanoreceptors and processed both bioelectrically and biochemically—locally (at tissue, cellular, and molecular levels) and systemically (throughout the integrated organism)—even though this study focuses solely on the discrete structure of the anatomical muscle model.

3. CONCLUSIONS

This study represents a significant contribution to the scientific understanding of tension transmission mechanisms in musculo-fascial structures, through the innovative integration of the photoelastic method in the field of manual therapy biomechanics. The systematic implementation of photoelasticity allowed for precise visualization of the spatial distribution of stresses in simulated anatomical structures, providing a robust methodological framework for the quantitative assessment of tissue response to various types of mechanical loading. The obtained results demonstrate the existence of a tension gradient dependent on both specific muscle geometry and insertion points, highlighting the differential propagation of stresses in the anterior and posterior fascicles of the deltoid muscle.

The developed methodology, which combines experimental approaches through physical modeling with advanced numerical analyses using the finite element method, has led to the identification of relevant structure-function correlations. The nonlinear relationship between the intensity of the applied mechanical stimulus and the optical response of the material was empirically demonstrated, with direct implications for understanding the mechanisms of action of Bowen Therapy at the tissue level. These findings provide an objective basis for optimizing therapeutic protocols and establishing scientific criteria for evaluating the effectiveness of manual interventions.

Despite these significant contributions, the study also highlights several methodological limitations that open avenues for future research. Among these are the need to improve physical models to more accurately replicate the viscoelastic and thixotropic properties of fascial tissue, as well as the integration of mechanobiological and neurophysiological aspects into the mechanical approach. The major challenge in translating these results into clinical practice lies in adapting the models to interindividual anatomical variability and incorporating hemodynamic and metabolic factors into mechanical simulations.

Future technological development perspectives include the implementation of smart materials with adaptive mechanical properties and the creation of advanced haptic platforms for simulating therapist-patient interactions. Future multiscale approaches should encompass modeling from the molecular level to that of the entire organism, with emphasis on mechanotransduction processes and electromechanical interactions in myofascial tissue. On the applied level, this research promises the personalization of manual interventions based on individual tension profiles and the development of therapeutic guidance-assisted systems.

Collectively, this interdisciplinary research establishes a benchmark in the study of manual therapies through advanced optomechanical methods, highlighting the need for a holistic approach that integrates anatomical complexity, physiological dynamics, and individual variability. The continuation of these investigations, with emphasis on clinical validation and methodological refinement, holds the potential to transform practices in rehabilitation and integrative medicine, paving the way for new paradigms in musculoskeletal disorder management. Investments in applied research within this field are justified both by the theoretical prospects of understanding pathophysiological mechanisms and by the practical benefits in optimizing therapeutic interventions.

4. REFERENCES

[1] Sciammarella, C.A., Sciammarella, F.M., *Experimental mechanics of solids*, John Wiley & Sons, Ltd, ISBN 978-0-470-68953-0, 2012.

[2] Kobayashi, A.S., *Handbook on experimental mechanics*, Second Edition, Society for Experimental Mechanics, ISBN 1-56081-640-6, 1993.

[3] Theocaris, P.S., Gdoutos, E.E., *Matrix theory of photoelasticity*, Springer-Verlag Berlin Heidelberg GmsH, doi 10.1007/978-3-540-35789-6, 1979.

[4] Hibbeler, R.C., *Mechanics of materials*, Sixth Edition, Pearson Prentice Hall, ISBN 0-13-191899-0, 2005.

[5] Chen, L., Zhang, M., Li, Y., *Visualization and quantification of the stress distribution on epoxy resin through photoelasticity and infrared radiation techniques*, AIP Advances 12, 015312, 2022, https://doi.org/10.1063/ 5.0074643.

[6] https://www.micro-measurements.com/ photostress-document-library

[7] Gherasim, D, M. Botean, I, A. Arghir, M., *Photoelasticimetry method used to highlight*

deformations of the left deltoid of the human body. Model creation, Acta Technica Napocensis, Series: Applied Mathematics, Mechanics, and Engineering Vol. 66, Issue III, 2023.
[8] Hansen, C., Taylor-Piliae, R.E., *What is Bowenwork? A Systematic Review*, The Journal of Alternative and Complementary Medicine, volume 17, no. 11, pp. 1001–1006, ª Mary Ann Liebert, Inc., 2011.
[9] Huang, C., at all, *Mechanotherapy: revisiting physical therapy and recruiting mechanobiology for a new era in medicine*, Trends in Molecular Medicine, volume 19, no. 9, pp. 555-564, 2013.
[10] Loghmani, M.T., Whitted, M., *Soft Tissue Manipulation: A Powerful Form of Mechanotherapy*, Physiother Rehabil 1: 122, 2016.
[11] Thompson, W.R., Scott, A., Loghmani, T., Ward, S.R., Warden, S.J., *Understanding Mechanobiology: Physical Therapists as a Force in Mechanotherapy and Musculoskeletal Regenerative Rehabilitation*, Phys. Ther, 96:560-569, 2016.
[12] Chaitow, L., *Fascial Dysfunction Manual Therapy Approaches*, Second Edition. Handspring Publishing. Edinburgh, 2018.
[13] Carter, B., *A pilot study to evaluate the effectiveness of Bowen technique in the management of clients with frozen shoulder*, Complement Ther. Med., 9, pp. 208–215, 2001.
[14] Carter, B., *Clients' experiences of frozen shoulder and its treatment with Bowen technique*, Complement Ther. Nurs. Midwifery, 8, pp. 204–210, 2002.
[15] Gherasim, D., Arghir, M., *Considerations of vibration action on the human body energetically point of view*, Acta Technica Napocensis, Series: Applied Mathematics, Mechanics, and Engineering, Vol. 59, Issue II, 2016.
[16] Argenbright, C.A., Taylor-Piliae, R.E., Loescher, L.J., *Bowenwork for symptom management of women breast cancer survivors with lymphedema: A pilot study*, Complementary Therapies in Clinical Practice, 25, pp. 142-149, 2016.
[17] Findley, W.T., *Fascia Research Perspectives*, International Journal of Therapeutic Massage and Bodywork, volume 2, no. 2, 2009.
[18] Botean, I.A., Takacs, I.A., Hărdău, M., *Photoelasticimetry applications in biomechanics*, Acta Technica Napocensis, Series: Applied Mathematics and Mechanics, Vol. 54, Issue I, 2011.
[19] https://tiedemann-instruments.de/ en/ photoelasticity
[20] Tripa, P., *Metode experimentale pentru determinarea deformaţiilor şi tensiunilor mecanice*, Editura Mirton, Timişoara, 2010.
[21] Schleip, R., Jäger H., Klingler, W., *What is 'fascia'? A review of different nomenclatures*, J. Bodyw. Mov. Ther., 16(4), pp. 496-502, 2012, doi: 10.1016/j.jbmt.2012.08.001.
[22] Stecco, C., Schleip, R., *A fascia and the fascial system*, Journal of Bodywork & Movement Therapies. Elsevier Ltd., 2015.
[23] Stecco, C. Schleip, R., *A fascia and the fascial system, Journal of Bodywork and Movement Therapies*, vol. 20, No. 1, pp. 139-140, 2016, doi:10.1016/j.jbmt.2015.11.012.

Răspunsul biomecanic al unui model de deltoid stâng la stimulii tehnicii Bowen

Rezumat: Acest studiu analizează distribuţia tensiunilor mecanice din muşchiul deltoid stâng folosind fotoelasticimetria, o metodă experimentală avansată bazată pe proprietatea de birefringenţă accidentală a materialelor optice active. Au fost create modele anatomice din răşină epoxidică (EP14NV) care reproduc geometria umană sănătoasă, simulând stimulii manuali specifici terapiei Bowen. Trei modele rigide (M1–M3) au fost încărcate static cu forţe cuprinse între 13,42 şi 28,12 N, iar câmpurile de tensiune au fost analizate cu ajutorul unui polariscop cu polarizare circulară. Rezultatele au evidenţiat modele distincte de franje izocromatice, stabilind o corelaţie cantitativă între magnitudinea forţei aplicate şi propagarea tensiunii în fasciculele anterioare şi posterioare. Studiul confirmă utilitatea fotoelasticităţii în modelarea biomecanică, deşi limitări precum absenţa viscoelasticităţii reale indică necesitatea îmbunătăţirii modelelor viitoare. Cercetarea demonstrează o corelaţie directă între intensitatea forţei şi răspunsul mecanic, sugerând game optime de presiune pentru aplicaţiile terapiei Bowen. Aceste concluzii validează fotoelasticimetria ca instrument de evaluare non-invazivă a terapiei musculară, deschizând noi perspective în analiza metodelor de tratament conservator.

Adrian Ioan BOTEAN, PhD. Eng., Lecturer, Mechanical Engineering Department, Faculty of Automotive, Mechatronics and Mechanical Engineering, Technical University of Cluj-Napoca, 28 Memorandumului, 400114 Cluj-Napoca, Romania, adrian.ioan.botean@rezi.utcluj.ro.
Dan Marius GHERASIM, PhD Student, Department of Mathematics, Technical University of Cluj-Napoca, str. L. Baritiu, nr. 27, Tel. 0747.408.381, dangherasim@yahoo.com.
Mariana ARGHIR, Em. Prof. PhD., Department of Mechanical Engineering Systems, Technical University of Cluj-Napoca, B-dul Muncii, No. 103-105, Tel. 0729.108.327, marianaarghir@yahoo.com.